Expert Opinion

Ultrasound targeted microbubble destruction for drug and gene delivery

Christian R Mayer, Nicolas A Geis, Hugo A Katus & Raffi Bekeredjian[†]
[†]*University of Heidelberg, Department of Internal Medicine III, 69120 Heidelberg, Germany*

Background: Gas-filled microbubbles have been used as ultrasound contrast agents for some decades. More recently, such microbubbles have evolved as experimental tools for organ- and tissue-specific drug and gene delivery. When sonified with ultrasound near their resonance frequency, microbubbles oscillate. With higher ultrasound energies, oscillation amplitudes increase, leading to microbubble destruction. This phenomenon can be used to deliver a substance into a target organ, if microbubbles are co-administered loaded with drugs or gene therapy vectors before i.v. injection. *Objective*: This review focuses on different experimental applications of microbubbles as tools for drug and gene delivery. Different organ systems and different classes of bioactive substances that have been used in previous studies will be discussed. *Methods*: All the available literature was reviewed to highlight the potential of this non-invasive, organ-specific delivery system. *Conclusion*: Ultrasound targeted microbubble destruction has been used in various organ systems and in tumours to successfully deliver drugs, proteins, gene therapy vectors and gene silencing constructs. Many proof of principle studies have demonstrated its potential as a non-invasive delivery tool. However, too few large animal studies and studies with therapeutic aims have been performed to see a clinical application of this technique in the near future. Nevertheless, there is great hope that preclinical large animal studies will confirm the successful results already obtained in small animals.

Keywords: drug delivery, gene therapy, microbubble, sonoporation, ultrasound

Expert Opin. Drug Deliv. (2008) 5(10):1121-1138

1. Introduction

Small air bubbles have been used since the late sixties to enhance ultrasound contrast [1]. These air bubbles do not circulate systemically after i.v. injection, due to their very short half-life and large size. Thus, new generation microbubbles (MB) were developed with shells, stabilizing the gas–liquid interface and low diffusive gases to increase the microbubble circulation time. Clinical ultrasound systems use these microbubbles to opacify blood-filled cavities and to visualize tissue perfusion. More recently, microbubbles have become an interesting tool in experimental gene and drug delivery. When sonified with ultrasound in their resonance, near or subresonance frequency [2-4], microbubbles oscillate. At higher ultrasound pressures, high amplitude oscillations result in microbubble destruction. This phenomenon can be used to locally and transiently increase cell membrane and capillary permeability. Thus, a bioactive substance loaded on the microbubble shell or co-administered with the bubbles can be selectively delivered to a target tissue. The safety of ultrasound has been widely studied, resulting in guidelines designed to control thermal and mechanical biological effects [5]. Given that ultrasonic destruction

informa healthcare

10.1517/17425240802418172 ISSN 1742-5247

of microbubble contrast agents can result in permeabilisation of surrounding membranes, insonification of these agents requires additional safety considerations. This review article will give an overview of various experimental and preclinical applications of microbubbles as vehicles for drugs or genes and will summarize the studies on safety aspects. Finally, we will discuss the future options of microbubbles, including their limitations as drug and gene carriers.

2. Properties of microbubbles

Using microbubbles as drug or gene delivery systems is a challenging task. Many parameters can be varied that will determine their successful therapeutic application, such as shell material, core gas, type of microbubble production, targeting ligand, the substance to be delivered and ultrasound modalities. However, this wide range of variables also allows different approaches to improve therapeutic microbubble applications. Very good review articles have been published on the physical behaviour of MBs and their dependence on the used compounds [6-8]. Thus, we will give here only a short summary on MB properties, and will concentrate more on concepts of microbubble design and studies delivering various substances to different tissues.

Microbubble composition: modern microbubbles have diameters between 1 – 5 μm and consist of two parts: a core with an inert and low soluble gas, such as perfluorocarbones, and a stabilizing shell that can consist of different materials, such as phospholipids, proteins (especially albumin) and polymers. Some microbubbles are partially filled with oil (soybean or coconut) to increase the payload of lipophilic substances [9-10].

Microbubble preparation: a variety of methods have been described to produce microbubbles. These comprise, among others, the mechanical agitation method [10], mainly used for the production of phospholipid-shelled microbubbles and acoustically active lipospheres; the emulsification method [11] for the production of polymer-shelled microcapsules and some phospholipid-shelled microbubbles; the probe-type sonication method, mostly used for protein-shelled microbubble construction; and the spray-drying method [12], which is a versatile approach to produce polymer-, protein- as well as phospholipid-shelled microbubbles.

The gas core: the first microbubbles were filled with air [13-16]. Air is highly soluble and can thus easily diffuse out of the microbubbles, leading to a short half-life after i.v. injection. Using heavy gases with low solubility, such as perfluorocarbones, increased the lifespan of MBs in blood significantly [17-22]. Other gases like nitric oxide (NO) have been tested as potential therapeutic gas cores, but did not show any additional benefit in the context of MB stability or drug and gene delivery [23].

The shell: many researchers use phospholipid shells. They form stable monolayer coatings of the gas core and offer a hydrophilic outer surface and a lipophilic inner surface.

Lipids can be chosen from a virtually unlimited library to optimise the binding of substances, such as drugs, genes, proteins and other compounds. Additionally, lipid shells are highly compliant and allow microbubble dilation and compression during ultrasound-induced oscillation. The lipid shell readily expands, ruptures, reseals, compresses, buckles and respreads with each acoustic cycle.

The first commercially available and approved MBs were albumin-coated (Albunex®, Molecular Biosystems, Inc., San Diego, USA and Optison™, GE Healthcare, Buckinghamshire, United Kingdom). Protein-shelled microbubbles have been developed to carry targeting ligands [24] and DNA [25,26]. These MBs can easily be modified and have a long half-life in the systemic circulation. They can bind substances after MB assembly, but have the disadvantage that only heat stable substances can be added before microbubble production [27].

Recently, polymer shells have been developed as a third shell type. Several investigators have used organic solvents to dissolve and disperse the polymer, followed by resuspension of lyophilized products to form hollow polymer capsules. This method has produced microbubbles with enhanced stability. However, chain entanglement and covalent bonds inherent in the polymer shells reduce microbubble compliance in the ultrasound field.

3. Drug delivery and drug loading of microbubbles

Various concepts have been described to deliver bioactive substances using ultrasound targeted microbubble destruction (UTMD) (**Figure 1**): (a) microbubbles can be manufactured together with a bioactive substance, thus potentially incorporating it into the microbubble shell or lumen; (b) microbubbles can be incubated with a bioactive substance, thus attaching the substance to the microbubble shell, presumably by electrostatic or weak non-covalent interactions; or (c) microbubbles and the bioactive substance can be co-administered, taking advantage of increased cell and capillary permeability only after UTMD [28]. Incorporating and attaching a substance has the additional advantage of protection against degradation or disintegration (as one would expect, e.g., for DNA in serum) after i.v. infusion [29,30].

On a more molecular level, various physicochemical concepts can be used to load bioactive substances on different MB types. Drug molecules can either be associated to the MB shell by means of electrostatic or hydrophobic interactions, or merely physical encapsulation (**Figure 2**). (A) Charged therapeutics (e.g., DNA, RNA) can be coupled electrostatically to the outer MB surface if cationic lipids or denatured proteins are used. (B) Amphiphilic molecules can penetrate into the monolayer of phospholipid–MBs. (C) Acoustically active lipospheres incorporate highly hydrophobic molecules in their inner oil layer. (D) Using

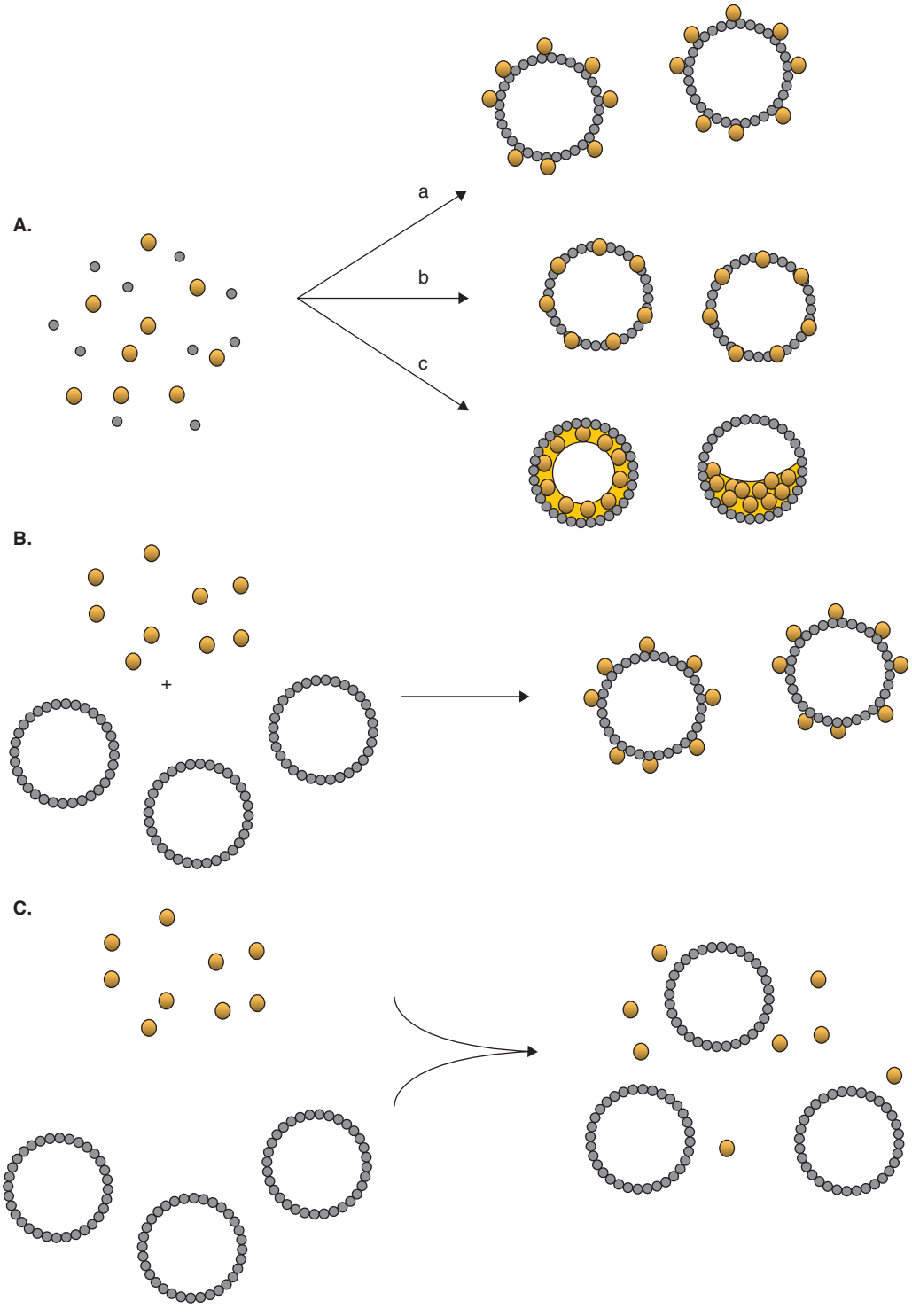

Figure 1. Different delivery concepts of therapeutic substances. A. Co-formation of microbubbles together with a bioactive substance: a. the substance adheres to the microbubble shell; b. the substance is incorporated into the microbubble shell; c. the substance is part of an inner oil layer. **B.** Incubation of microbubbles with a bioactive substance leading to attachment onto the surface. **C.** Co-injection of microbubbles and the bioactive substance.

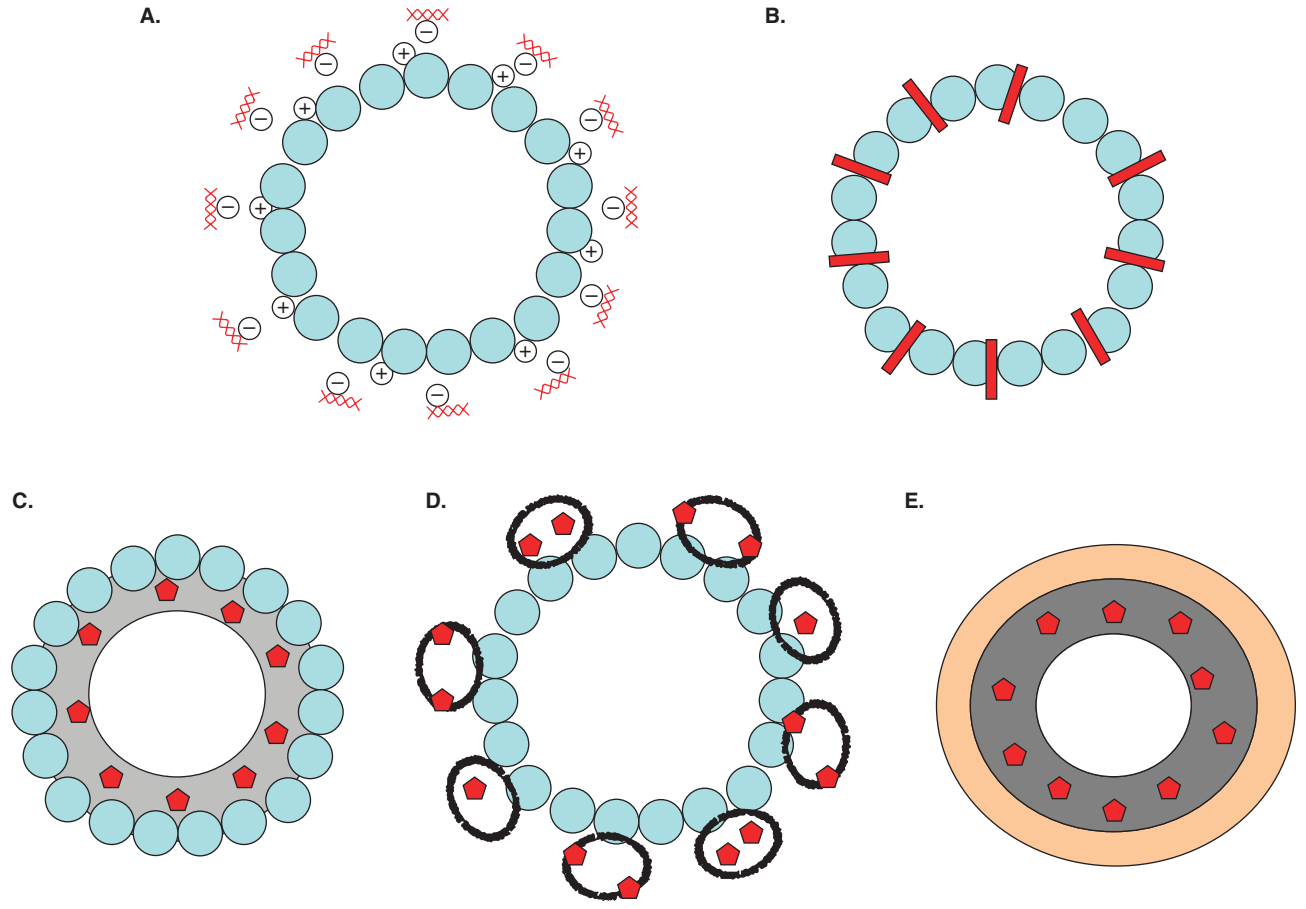

Figure 2. Molecular mechanisms of different loading concepts of therapeutic substances. A. Coupling of charged therapeutics by electrostatic interaction. **B.** Penetration of amphiphilic molecules into the monolayer of phospholipid microbubbles. **C.** Incorporation of hydrophobic molecules in an inner oil layer of acoustically active lipospheres. **D.** Secondary carrier-associated microbubbles binding nanometer-sized particles with the payload. **E.** Double emulsification microbubbles encapsulating molecules into shells of biodegradable polymer coated with a biocompatible material.

secondary-carrier associated MBs, the payload is attached to nanometer-sized particles (e.g., liposomes, lipoplexes), which on their turn can be associated with MBs. This approach may increase both loading capacity and transfection efficacy [31]. (E) Encapsulation of drug molecules into shells of biodegradable polymers coated with a biocompatible material (e.g., gelatine) is a feasible approach relatively irrespective of the nature of the drug. These MBs are also referred to as 'double emulsification microcapsules'.

The effective carrying capacity of MBs is limited to their shell. Compared to phospholipid MBs (2 – 3 nm, [32]) polymer microcapsules (50 – 200 nm, [33]), protein-shelled MBs (200 – 300 nm, Molecular Imaging and Contrast Agent Database [34]) and especially acoustically active lipospheres are endowed with rather thick shells. For instance, Unger *et al.* has developed thick-shelled lipospheres with a shell strength of up to 500 nm, offering a much larger volume [35]. Other groups developed partially oil-filled MBs with an even higher payload [10]. Borden *et al.* demonstrated an approach to increase the loading capacity of MBs for plasmid DNA over tenfold by a multiple layer technique [36]. By using a formulation approach allowing entire shell volume loading, Frenkel *et al.* achieved about a 200-fold increased loading of pDNA on albumin MBs [25].

In general, many different types of therapeutic substances can be used in the context of UTMD: drugs, small molecules and gene therapy vectors. Most studies that have been performed with microbubbles as carriers for bioactive substances have used gene therapy vectors. There are several reasons for this. First, using a gene therapy vector, only one application may be required to achieve a therapeutic response, whereas most drugs would need repetitive applications. Second, a rather low payload can suffice for a therapeutic response, since expression of the transgene will augment its effect. Third, while most drugs can be systemically administered, gene therapy vectors mostly have to be locally administered.

Using drugs, proteins or small molecules, various aspects have to be considered. The bioactive substance should be chemically compatible with the microbubble shell, it should have a sufficient effect in low concentrations and it should suffice to deliver the substance only a few times (optimally just once).

Since gene therapy vectors are most important in experimental UTMD studies we will briefly describe the two most important groups of vectors that are used in gene therapy.

Plasmid DNA can carry large genes (> 50 kB), is cheap in production, has low immunogenic properties, low toxicity, is heat stable and water soluble. Loading of MBs with DNA is easy and efficient. However, this is outweighed by low transfection efficiency due to the inability to enter cells without help and only transient expression due to intracellular degradation, limiting the efficiency of the vector.

Viral vectors offer additional advantages compared to plasmid DNA. Due to active targeting and cell penetration, higher transduction efficiencies can be achieved. There are primarily four types of viruses in use for gene therapy: adeno-, adeno-associated-, lenti- and retroviruses, all with different advantages and disadvantages. The first two of these vectors have been predominantly used in UTMD application. Adenoviral vectors are limited by their potential to induce strong immune reactions and hepatic tropism.

Adeno-associated virus vectors show only minimal immunogenicity, no direct toxicity and long-term transgene expression for up to 2 years. Different serotypes show different cell tropism. Disadvantages include limitations in high-titer vector production and limited packaging capacity of only 4.8 kB [37].

4. Targeting

Molecular ultrasound imaging uses targeted microbubbles to selectively enhance ultrasound contrast of specific endothelial structures. Current developments in this field have been recently reviewed by Dyton and Rychak [38]. These ideas have been implemented to increase specificity in UTMD. The basic strategy to target MBs is to couple covalent or non-covalent targeting ligands to the shell [39-42]. Specific ligands, such as monoclonal antibodies, receptors, glycoproteins, carbohydrates, peptides or peptidomimetics have been used. For successful targeting of a disease-related molecule, several factors have to be considered. The targeted molecule should be sufficiently specific for the disease process and should not be expressed constitutively in significant amounts. Also, the target should be found at the inner blood vessel surface. Attachment of microbubbles happens in the face of vascular flow, and thus factors like shear rate in the tissue of interest, ligand density on the microbubbles, bond affinity of the ligand and target molecule density have to be considered.

Coupling of a targeting ligand to the MB surface can either be achieved by a direct covalent bond or through biotin–avidin linkage (**Figure 3**). Due to immunogenic properties the latter is primary useful for proof-of-concept and preclinical targeting studies. With regard to possible clinical applications, covalent attachment is more desirable. Coupling strategies include binding of an amino group of the ligand to a carboxyl group on the MB shell. Alternatively a thiol group of the ligand can be coupled to a maleimid group on the MB shell, forming a strong thioether bond. By applying a separating flexible spacer arm (e.g., polyethylenglycol, PEG) between the targeting ligand and the MB surface, bubble affinity and shear resistance can be improved [43]. To account for immunogenic effects of ligand-labelled MBs, Borden *et al.* presented a very sophisticated targeting surface model concealing the ligand by a polymeric overbrush of, for example, PEG. By applying ultrasound radiation force, local revelation of the targeting ligand can be achieved [44].

5. Safety

During normal diagnostic ultrasound, thermal and non-thermal effects can be observed, without any confirmed adverse biological effects on patients. Diagnostic ultrasound is therefore considered to be a safe technique. With the introduction of MBs as ultrasound contrast agents in the 1980s, new safety concerns emerged and the effects of ultrasound in combination with contrast agents were extensively evaluated after intracoronary and i.v. injection. No clinically relevant side effects were detected under diagnostic conditions [15,45]. Nevertheless, safety concerns of diagnostic MB applications are a present issue with the US FDA.

Haemorrhages [46-49], haemolysis [50], opening of the blood–brain barrier (BBB) [51] and endothelial cell death [52] could be induced in animal models by MB destruction with high acoustic energies. These effects showed to be strictly dose and ultrasound energy dependent and are part of the mechanisms proposed for a successful gene or drug delivery. Nevertheless, they have to be monitored for possible side effects in a therapeutic concept.

6. Targets

A new drug delivery system has to compete with current drug delivery approaches. Ultrasound targeted microbubble destruction could be an interesting option for drug delivery of highly toxic substances, thus having high local concentrations in the target organ, while keeping systemic concentration low. Furthermore, it may be used for the penetration of capillary barriers to access pharmacological sanctuaries in organs like the brain and testes. Finally, it could be used to deliver substances non-invasively that would normally be unable to reach their destination (such as

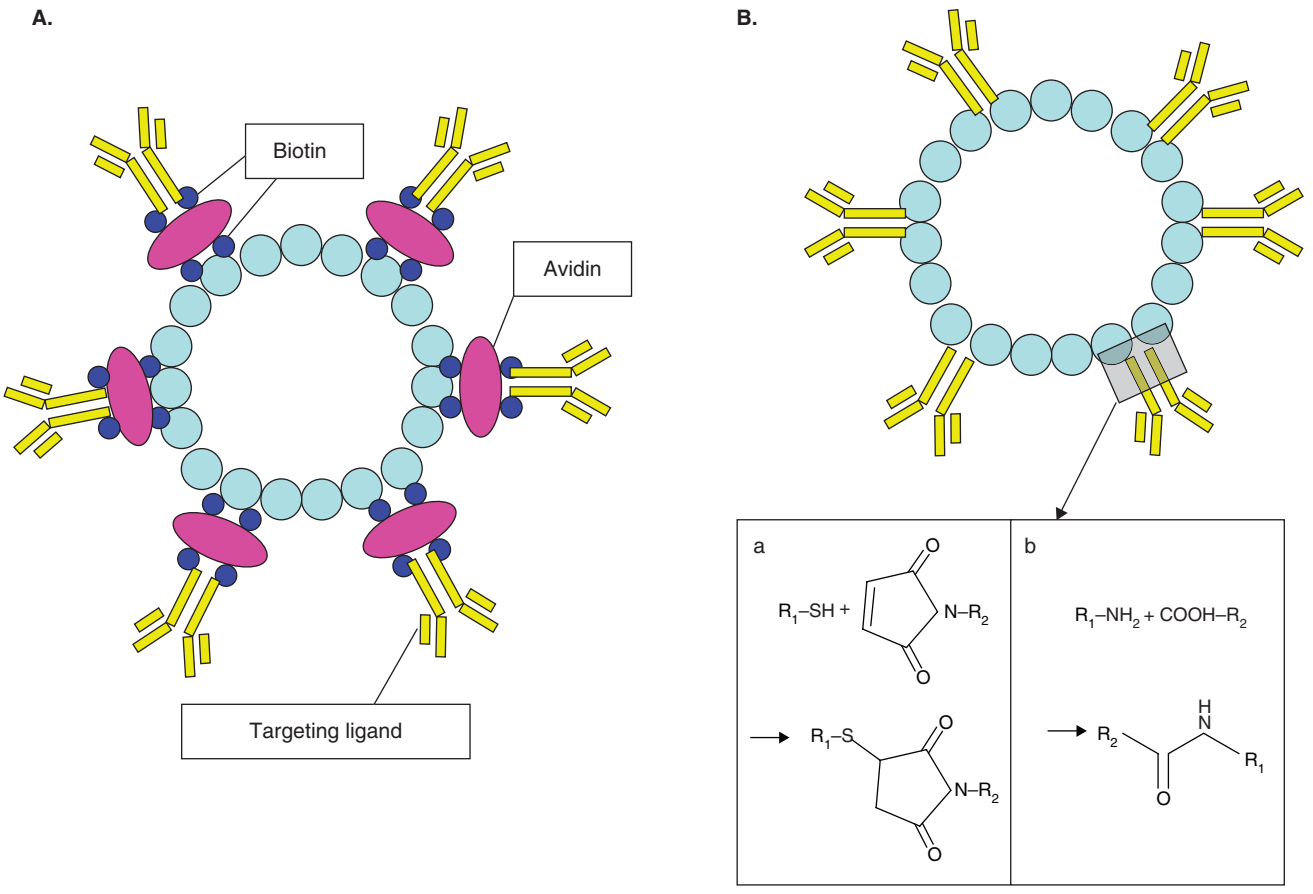

Figure 3. Different concepts for coupling of a targeting ligand to the microbubble surface. A. Biotin–avidin linkage: a biotinylated ligand is coupled to a biotinylated microbubble via an avidin bridge. **B.** Covalent coupling: (a) by binding of a thiol group of the ligand to a maleimid group on the microbubble shell; or (b) an amino group of the ligand to a carboxyl group on the microbubble shell.

in gene therapy). Taking these aspects into account, a few main target organs emerged as the focus of UTMD applications: i) the cardiovascular system with a focus for gene therapy; ii) the central nervous system for small molecule delivery; and iii) tumour therapy to reduce systemic side effects of cytotoxic drugs.

6.1 Cardiovascular system

Ultrasound targeted microbubble destruction is a promising method for the cardiovascular system. Cardiac applications have been among the first and most intensively studied in this field of research [28]. This is due to the origin of this technique (myocardial contrast echocardiography), the accessibility of the heart, the high capillary density of the myocardium, the availability of appropriate echocardiography machines and the isolation of the heart by surrounding lung tissue (that would not be accessible for UTMD). In addition, cardiovascular diseases are the leading cause of mortality and morbidity in developed countries. Advances in pharmaceutical, interventional and surgical therapies have already improved the survival and quality of life of patients suffering under cardiac diseases, but due to the medical and economical significance, further improvements are necessary and motivate new therapeutic options in cardiology.

In the cardiovascular set-up, drugs play an important role but systemic toxicity is a minor issue. Therefore, there is little interest in establishing targeted drug therapies for the heart.

Gene therapy has been considered as a promising new therapeutic concept for these patients. However, so far only highly invasive techniques have been able to deliver gene therapy vectors with high local concentrations and transfection rates to the heart. Ultrasound targeted microbubble destruction could meet these needs by combining low invasiveness with higher gene transfer efficiency, as well as high organ specificity.

Protein delivery could bypass the complex processes of gene therapy such as transfection, regulation and expression by direct application of the therapeutic protein. Again a targeted release with a high local concentration and capillary permeability would be beneficial, but the low duration of the protein effect would limit their application.

6.1.1 *Gene delivery*

Around 2000 first experiments with reporter gene constructs targeting cardiovascular tissue have been published [53,54]. These demonstrated that plasmid DNA or adenovirus in combination with UTMD can significantly increase gene expression in the targeted organ (**Table 1**). After these first encouraging experiments, a series of different approaches have been performed in rodents to further increase transfection efficiency by varying experimental parameters, such as ultrasound conditions, vector and MB type. All experiments showed the superiority of UTMD compared to simple vector (plasmid DNA, virus, siRNA) injection. While some researchers could detect mild tissue damage, such as haemorrhages, no permanent damage was seen. The next generation of experiments used potentially therapeutic constructs, thus moving closer to preclinical studies. Angiogenesis is one of the most interesting clinical targets in the field of cardiovascular diseases and several groups tried to induce growth of a new vessel. Taniyama *et al.* used hepatocyte growth factor (HGF) as plasmid DNA bound to Optison in a rat ischemic skeletal muscle model and could induce collateral development [55]. Kondo *et al.* could reduce infarct size and enhance angiogenesis in a rat myocardial infarction model with the same approach [56]. Similar results were shown by Li *et al.* [57]. Different forms of vascular endothelial growth factor (VEGF) plasmid DNA in combination with UTMD transiently induced angio- and arterio-genesis in rat hearts [58,59] or limbs [60]. Other targets were inhibition of neointimal growth [61-63] or heart failure [64,65].

Despite this range of therapeutic experiments, most studies were limited to small animal models and suboptimal vectors. Future efforts have to include large animal models and improved vector systems for efficient gene therapy.

6.1.2 *Protein delivery*

Applying active proteins to the cardiovascular system would bypass the difficulties of vector delivery and transgene expression. Albumin MB bound VEGF was successfully delivered to the heart. A 13-fold augmentation of cardiac VEGF uptake was seen compared to systemic VEGF administration [66]. Another study using lipid microbubbles with luciferase protein demonstrated a sixfold to sevenfold augmented cardiac uptake of luciferase, compared to systemic administration, in rats [67]. Iwasaki *et al.* showed that recombinant HGF could be co-injected with Optison, improving heart function in a heart failure mouse model [65]. The repetitive application could even further improve cardiac contractility. However, due to the high costs for recombinant proteins and their short half-life, protein delivery by UTMD is rather irrelevant in a clinical setting.

6.2 Central nervous system

The BBB protects neurons of the central nervous system by a tight layer of endothelial cells from pathogens and toxins. At the same time, this eludes neurons from many drug therapies [68]. A lot of effort has been undertaken to increase the permeability of the BBB to facilitate delivery of drugs into the brain without a clinically applicable method being produced [69-73].

Ultrasound is an important tool to assess intracerebral blood flow in humans, and the addition of contrast agents helps to increase its diagnostic potential [74]. Thus, studying the therapeutic potential of UTMD in the central nervous system is warranted.

Vykhodtseva *et al.* demonstrated 1995 that high power ultrasound could open the BBB in rabbits [75]. However, haemorrhage and tissue damage was also observed in this first experiment. They used a rabbit model, with partial removal of the skull to get a free acoustic path for UTMD with Optison. The head of the animal was positioned on a magnetic resonance imaging (MRI) coil and BBB permeability was detected by extravasation of an MRI contrast agent. The ultrasound parameters have been varied during multiple subsequent experiments with the aim of reducing tissue damage and haemorrhage while obtaining an optimal BBB opening (**Table 2**). Different ultrasound thresholds were identified for BBB disruption and tissue damage. The optimal parameters seemed to be around 1 MHz and peak pressures were between 0.2 and 1 MPa [76-79]. Various studies proved that BBB opening would allow deposition of macromolecules, such as immunoglobulins and horseradish peroxidase [80-82]. Furthermore, four mechanisms were identified as likely mechanisms for macromolecule passage through the BBB after UTMD: i) transcytosis; ii) transendothelial fenestration; iii) widening of tight junctions; and iv) passage through destroyed endocytes [76-83]. Recently, targeted deposition of doxorubicin in a rat brain tumour model demonstrated a possible therapeutic approach [84].

Other groups have demonstrated comparable results for BBB opening through UTMD with Sonovue® (Bracco, Milan, Italy) [85] and in a mouse model with intact skull [86,87].

The concept of opening the BBB by UTMD is intriguing. However, suboptimal accessibility in humans due to the skull will remain a major problem. Only with invasive strategies, such as partial removal of the skull, will unlimited access to the brain be possible. Again, large animal experiments are necessary for future preclinical studies.

6.3 Tumour targeting

Over the last decades, the survival of patients with cancer has steadily increased. One of the major aspects leading to this development has been the successful combination of different therapeutic modalities, such as surgery, radiation and adjuvant or neoadjuvant chemotherapy. The aggressiveness of chemotherapeutic strategies is mainly limited by side effects, due to the systemic application of these drugs.

Ultrasound targeted microbubble destruction is an interesting and promising tool to increase the organ or

Table 1. Gene transfer in the cardiovascular and musculoskeletal system.

Ultrasound conditions	Microbubbles	Gene	Model	Results	Ref.
1.3 MHz, MI 1.6, PW, ECG triggered	Optison	1.0×10^{10} pfu/ml β-Gal Adenovirus	Rat myocardium	10-fold higher expression in US treated myocardium than in control group. Different sound settings showed optimal expression at 1.3 MHz, PW, MI 1.6, ECG triggered	[53]
956 kHz, MI 2.0, ECG triggered, 60 sec	Optison	Luciferase plasmid DNA	Human vascular smooth muscle cells	300-fold higher gene expression compared to plasmid DNA without US	[54]
1.3 MHz, MI 1.5 – 1.7, PW, ECG triggered	Cationic lipid MBs	6, 5 μg/kg chloramphenicol acetyltransferase	Dog heart	Only cardiac CAT expression in US and MB treated group. Local distribution with predominantly apical expression	[115]
2.2 MHz, 1.2 MI, CW, 30 sec	Optison	20 μg β-Gal and eNOS plasmid DNA	Rat carotide	30-fold higher β-Gal activity and enhanced NO-mediated relaxation	[116]
1 MHz, 2.5 W/cm^2, 1 min	Optison	20 μg luciferase and β-Gal plasmid DNA	Rat limb	15-fold higher expression of luciferase after UTMD compared to plasmid injection without MBs and US	[55]
1.3 MHz, MI 1.6 – 2.0, PW, ECG triggered, 20 min	Liposome MBs	600 μg luciferase plasmid DNA	Rat myocardium	Expression equivalent to 0.25×10^{12} adenoviruses with localized activity in the myocardium	[117]
1.3 MHz, MI 1.5, PW, ECG triggered, 20 min	Optison and lipid MBs	350 μg luciferase plasmid DNA	Rat myocardium	Luciferase activity after 28 days peaked at days 2 – 4 with almost no activity outside the targeted region	[118]
1 MHz, 2.5 W/cm^2, 1 min	Optison	2 ng/g tissue HGF plasmid DNA	Chronically ischemic rat skeletal muscle	Augmentation of collateral vessel development as assessed by angiography on day 30	[63]
1 MHz, 2.5 W/cm^2, 2 min	Optison	50 μg p53 plasmid DNA	Post-angioplastic neointimal proliferation in rat carotide	Fivefold higher expression of p53 compared to control correlated with reduced neointimal proliferation	[63]
1.7 MHz, MI 0.9 – 1.7, PW, 3 min/1.0 MHz, 0.32 – 0.41 MI, CW, 3 min	Optison	100 μg luciferase plasmid DNA	Rat limb	US, MBs and 100 μg DNA showed 10-fold higher expression compared to plasmid alone, fivefold higher compared to plasmid and lipofectamine and twofold lower compared to 6×10^9 adenovirus	[119]
1.75 MHz, MI 1.9, PW, pulse every 7 sec for 15 min	Cationic lipid MBs	20 – 100 μg luciferase plasmid DNA	Rat limb	200-fold higher activity after intra-arterial versus i.v. injection, similar to direct intra-muscular injection	[120]
1 MHz, 2 W/cm^2, PW, 50% DC, 2 min	Optison	25 μg luciferase plasmid DNA	Mouse limb	Tenfold higher expression with Optison contrast agent compared to Levovist, Albunex and plasmid without MBs after direct intra-muscular injection	[121]
1 MHz, 3 W/cm^2, PW, 20% DC, 60 sec	Optison	10 μg GFP plasmid DNA	Mouse limb	30-fold higher expression compared to plasmid alone after direct intra-muscular injection	[122]
1 MHz, 0.6 W/cm^2, 15 min	Optison	100 μg TNF-α siRNA	Post-ischemic inflammation in rat myocardium	siRNA application prior to cardiac ischemia could reduce TNF-α expression and subsequently post-ischemic inflammation. Intra-vetricular injection was more effective than i.v.	[123]

BM-MNCs: Bone marrow-derived mononuclear cells; BR14: ; CAT: Chloramphenicol acetyltransferase; CW: Continuous wave doppler; DC: Duty cycle; ECG: Electrocardiogram; GFP: Green fluorescent protein; HGF: Hepatocyte growth factor; LV: Left ventricle; MB: Microbubble; MI: Mechanical index; NO: Nitric oxide; PW: Pulsed wave doppler; siRNA: Small interfering RNA; TIMP: Metalloproteinase inhibitor; TNF: Tumor necrosis factor; US: Ultrasound; UTMD: Ultrasound targeted microbubble destruction; VEGF: Vascular endothelial growth factor.

Table 1. Gene transfer in the cardiovascular and musculoskeletal system (continued).

Ultrasound conditions	Microbubbles	Gene	Model	Results	Ref.
1.3 MHz, MI 1.5, PW, ECG triggered, 2 min	Optison	60 µg luciferase and β-Gal plasmid DNA	Mouse myocardium	Eightfold higher gene expression with MBs compared to plasmid only	[124]
1 MHz, 2.5 W/cm^2, 2 min	Optison	100 µg E2F decoy	Post angioplastic neointimal proliferation in rat carotide	Significant reduction of neoitimal proliferation	[61]
1.3 MHz, PW, 2.1 kPa, ECG triggered, 2 – 4 min	Optison	1500 µg HGF plasmid DNA	Myocardial remodelling post-myocardial infarction in rat model	Effective gene expression after i.v. injection resulted in enhanced angiogenesis, limited infarction size, and prevented LV remodelling 3 weeks after MI	[56]
1.8 MHz, PW, ECG triggered	Optison	2000 µg $VEGF_{121}$ plasmid DNA	Angiogenesis after myocardial infarction in rat model	Significant higher expression of transfected plasmid	[59]
1 MHz, PW, 10 – 50% DC, 1.0 – 2.0 W/cm^2, 60 sec	BR14	500 µg luciferase, β-Gal and GFP plasmid DNA, GFP siRNA	Mouse myocardium	LV injection showed 60-fold higher expression than i.v. injection. Co-administration of siRNA could prevent GFP expression	[125]
1 MHz, PW, 20% DC, 2 W/cm^2, 30 sec	Optison and Sonovue	10 µg GFP plasmid DNA	Mouse limb	Threefold higher expression with Optison and Sonovue after direct intra-muscular injection	[126]
1 MHz, CW, 1.5 W/cm^2, 3 × 10 sec	Optison	10 µg HGF recombinant protein	Doxorubicin induced cardiomyopathy in mouse model	Protein induces proliferation and differentiation of cardiac progenitor cells and improves LV contractile function	[65]
1.3 MHz, PW, MI 1.6, ECG triggered, 20 min	Optison	120 µg $VEGF_{165}$ plasmid DNA	Angiogenesis in rat myocardium	Effective gene expression with increased capillary and arteriolar density within the myocardium 10 days after injection with regression 30 days after injection	[58]
1 MHz, PW, 6% DC, 1.8 MI, 2 min	BR14	33 µg/ml TIMP-3 plasmid DNA	Prevention of porcine saphenous vein graft failure	Lumen and total vessel area significantly greater in the TIMP-3 group compared to controls	[127]
1 MHz, 50% duty ratio, 2.0 W/cm^2 90 sec	Optison	1 × 10^8 BM-MNCs	Heart failure in hamster cardiomyopathy model	Delivery of BM-MNCs leading to increased capillary density and prevented cardiac remodelling	[64]
1.3 MHz, PW, MI 1.0, 10 min every 5 sec	Cationic lipid MBs	500 µg $VEGF_{165}$ plasmid DNA	Chronically ischemic rat skeletal muscle	Improvement in microvascular blood and vessel density	[60]
1.6 MHz, MI 1.3	Phospholipid MBs	HGF plasmid DNA	Rat myocard infarct model	UTMD delivered HGF into the infracted myocardium and produce an angiogenesis effect	[57]

BM-MNCs: Bone marrow-derived mononuclear cells; BR14: ; CAT: Chloramphenicol acetyltransferase; CW: Continuous wave doppler; DC: Duty cycle; ECG: Electrocardiogram; GFP: Green fluorescent protein; HGF: Hepatocyte growth factor; LV: Left ventricle; MB: Microbubble; MI: Mechanical index; NO: Nitric oxide; PW: Pulsed wave doppler; siRNA: Small interfering RNA; TIMP: Metalloproteinase inhibitor; TNF: Tumor necrosis factor; US: Ultrasound; UTMD: Ultrasound targeted microbubble destruction; VEGF: Vascular endothelial growth factor.

Table 2. Brain applications.

Ultrasound conditions	Microbubbles	Reporter	Model	Results	Ref.
1.63 MHz, 4.7, 3.3, 2.3 and 1.0 MPa, burst length of 100 m, repetition frequency of 1 Hz	Optison	Magnevist® (Schering, Berlin, Germany)	Rabbit brain	Sonications produced focal BBB opening without visible damage to the tissue at 1.0 MPa but neuronal loss at 2.3 MPa	[76,83]
1.63 and 1.50 MHz, 1 – 3 MPa, burst length of 100 min, repetition frequency of 1 Hz	Optison	Magnevist, Tryphan blue, IgG	Rabbit brain	US-induced BBB disruption and IgG passage via several routes	[82]
690 kHz, 3.1 MPa, 10-min exposure, repetition frequency of 1 Hz for 20 sec	Optison	Magnevist, horseradish peroxidase	Rabbit brain	BBB disruption is possible at a frequency of 0.69 MHz with minimal damage to the exposed brain parenchyma cells	[80]
260 kHz, 0.1 – 0.9 MPa, repetition frequency of 1 Hz for 20 sec	Optison	Magnevist	Rabbit brain	The threshold for BBB disruption was approximately 0.2 MPa	[77]
0.69 MHz, 0.6 – 1.1 MPa, 10-min exposure, repetition frequency of 1 Hz for 40 sec	Optison	Anti-dopamine D4 IgG	Mouse brain	Positive staining for dopamine D4 receptors in mouse brains after BBB opening	[81]
1.525 MHz, 0.5 – 1.1 MPa, burst duration: 20 min, duty cycle: 20%, durations: 2 – 4 shots, 30 sec per shot, 30 sec interval	Optison	Omniscan	Mouse brain	Opening of BBB through intact skull without microscopic tissue damage by UTMD possible	[86]
1.5 or 1.7 MHz, 0.36 – 2.5 MPa, burst length of 10 min, pulse repetition frequency of 1 Hz	Optison	DOX coinjected with MBs	Rat brain tumour model	Delivery of therapeutic concentrations of DOX to the targeted area	[84]
1 MHz, 0.9 and 1.2 MPa, burst length 10 min, 1% duty cycle, repetition frequency of 1 Hz, 30-sec duration	Sonovue 0, 30, 60 and 90 µl/kg	Evans blue	Rabbit brain	A higher dose of MBs results in more EB staining	[85]
1.5 MHz, 0.8 – 2.7 MPa, 20% duty cycle	Optison	Omniscan	Mouse brain	Region of the brain where BBB opening occurred increased with the pressure amplitude	[87]
2.04 MHz, 0.3 – 2.3 MPa, 20-sec duration; burst length: 10 min; pulse repetition frequency: 1 Hz	Optison	Magnevist	Rabbit brain	BBB disruption threshold has a frequency dependence consistent with the assumption underlying the MI	[79]
0.69 MHz, 0.1 – 1.5 MPa, burst: 0.1, 1, 10 min, pulse repetition frequency: 0.5, 1, 2, 5 Hz, duration: 20 sec	Optison dosage 50, 100, 250 µl/kg	Magnevist	Rabbit brain	No dependence of BBB opening on MB concentration or pulse repetition frequency	[78]

BBB: Blood–brain barrier; DOX: Doxorubicin; EB: Evans blue; MB: Microbubble; MI: Mechanical index; US: Ultrasound; UTMD: Ultrasound targeted microbubble destruction.

tissue specificity of chemotherapy by increasing vascular permeability in the tumour and releasing the drug at high local concentrations.

Four concepts have primarily been used to combine chemotherapeutics with MBs: i) coadministration of a drug with MBs [84,88-90]; ii) modified MBs with a thick lipid shell or partial lipid core loaded with a drug [9,10,35,91-93]; iii) MBs linked to drug-loaded lipospheres [94]; and iv) drugs incorporated inside the non-permeable shell of a biodegradable polymer [95-98].

The first studies with drug-loaded MBs were made by Unger *et al.* with Paclitaxel, a hydrophobic drug with a strong mitosis-inhibiting effect. Soybean oil-filled phospholipid MBs loaded with Paclitaxel were tested for cytotoxicity with HeLa cells and for toxicity in mice. The results showed a 100-fold lower toxicity in mice with a comparable cytotoxic effect in HeLa cells compared to free Paclitaxel [35]. The commercially available contrast agent Sonovue was used to reduce the LD_{50} of camptothecin on HeLa cells by 70% when co-administered and irradiated with ultrasound of 1 MHz and 270 J/cm^2 [99]. The effect of ultrasound targeted microbubble destruction was investigated with Evans Blue, demonstrating a significant but transient increase in vascular permeability for small molecules [100] and for large 8.5-nm diameter fluorescein isothiocyanate-labelled dextran molecules [101].

Various *in vivo* studies showed the potential of ultrasound targeted microbubble destruction in tumour therapy (**Table 3**): Tartis *et al.* used a similar type of MBs as Unger *et al.* but combined them with ligands targeting the αvβ3 integrin. Ultrasound and molecular targeting was successfully used to deliver Paclitaxel to the endothelium and interstitium of chicken chorioallantoic membrane vasculature *in vivo* [93]. Sonoda *et al.* co-injected bleomycin (BLM) with Optison in two mouse tumour models. The combination of bleomycin and ultrasound alone could reduce the dose for tumour regression to 0.5 mg/ml and with the addition of MBs to 0.06 mg/ml in a murine eyelid tumour model [102]. Iwanaga *et al.* found a complete regression of gingival squamous carcinoma cell tumours in nude mice treated with BLM and sonoporation [90]. A complete inhibition of tumour progression in a murine breast cancer model was induced by Gao *et al.* using copolymer MBs encapsulating Doxorubicin in combination with ultrasound [96].

These studies clearly demonstrate the therapeutic potential of UTMD-mediated chemotherapy delivery to tumours. Basically, any solid, ultrasound accessible and well perfused tumour can be used for this approach. An evaluation of systemic side effects due to microbubbles that have not been destroyed in the tumours is still missing in most experiments. This is one of several aspects that remains to be investigated before advancing to preclinical studies.

6.4 Gene delivery to other systems

The outlook of UTMD in cardiovascular gene therapy motivated the first experiments in other organ systems with green fluorescent protein (GFP) and Luciferase (Luc) as reporter constructs (**Table 4**). Shimamura *et al.* increased Luciferase expression by tenfold in the brain [103] and 60-fold in the spinal cord [104] of rats, which was also found by Takahashi *et al.* [105]. Increased GFP and Luc gene expression could be induced in ocular models [106,107], the liver [108], intervertebral discs [109], kidney [110], the intraperitoneal cavity (with Smad 7 as transgene) [111] and even lung [112]. Although different organs were targeted, the experiments showed similar characteristics. All of them used plasmid DNA, mainly in combination with the albumin MB Optison. Only a few publications describe an ultrasound-enhanced gene transfer in a disease model. Ka *et al.* was able to improve proteinuria, renal function and pathology in a murine autoimmune glomerulonephritis model by Smad 7 gene transfer [113]. Chen *et al.* targeted the pancreas with betacellulin and pancreatic duodenal homeobox-1 plasmid DNA to restore insulin production in a diabetic rat model [114]. These studies demonstrate that UTMD can be universally applied for various organs, diseases and with various bioactive substances.

7. Expert opinion

7.1 State of the art

Nearly a decade has passed since the first experiments were successfully performed, using microbubbles and ultrasound to deliver bioactive substances to specific organs. During this time, a considerable number of experimental studies have been published, targeting nearly any ultrasound accessible organ, delivering drugs, proteins, nucleotides and viruses as bioactive substance and using different microbubble types, as well as different loading/co-administration strategies. In addition, a remarkable number of review articles has been written, one of which being this very article, demonstrating the fascination and importance of this evolving technology. Why has ultrasound targeted microbubble destruction become such a prospering research field? The technique combines several unique aspects that have been demanded by increasing knowledge of basic science. While classic drug therapy, mainly using systemic administration of the therapeutic substance, will still form the major part of non-invasive treatment, basic research has come up with thousands of potentially therapeutic substances that cannot be administered as pills or injections. For those substances, targeted delivery systems are necessary, due to the toxic effects in non-target sites and/or very high production costs, making it unaffordable to systemically administer those new drugs. In addition, many of these new potentially therapeutic substances cannot enter the target sites unaided. This applies to naked DNA or inhibitory oligonucleotides and RNA. But even with some conventional drugs, local but non-invasive delivery would be beneficial, as in tumour therapy. Looking at these demands in modern pharmaco- and gene therapy, microbubbles seem to be an

Table 3. Tumor applications.

Ultrasound conditions	Microbubbles	Drug	Model	Results	Ref.
2.5 MHz, ± 100 kHz CW or 100 kHz PW, 0.8 W/cm^2	MRX-552 lipospheres	Paclitaxel in oil-filled MBs	HELA cells Toxicity studies in mice	Paclitaxel is soluble in oil-filled MBs and shows good cytotoxicity	[35]
1 or 3 MHz, 1.2, 1.7 or 1.8 W/cm^2	Biodegradable diblock copolymers	FITC and DOX	Mouse ovarial carcinoma model	Higher uptake in sonicated tumors	[98]
1 MHz, 1.0 W/cm^2, duty cycle 10%, 30 sec	Optison	MTX	Rabbit arthritis model	US treatment promotes uptake of MTX into synovial cells, resulting in acceleration of anti-inflammatory effects	[128]
2 MHz, 950 kPa, six 5-cycle pulses	Phospholipid MBs targeting $\alpha v\beta 3$ integrin	Paclitaxel in oilfilled MBs	Chorioallantoic membrane model	Successful targeting and drug delivery	[93]
1 MHz; 0.5 – 2 W/cm^2, 120 sec, duty cycle, 50%	Optison	Bleomycin 0.06 mg/ml and 0.5 mg/ml	Mouse eyelid tumor model	Ultrasound and MB promote efficient bleomycin uptake by cells	[102]
5 MHz, 1.9 MPa	Biotin/streptavidin conjugated phospholipid MBs and lipospheres	NBD-cholesterol in conjugated liposomes	Human prostate cancer cell	NBD–cholesterol could be transferred by UTMD *in vitro*	[94]
1 MHz	Phospholipid MBs with coconut filling	Resveratrol in oilfilled MBs		Oil-filled MBs show a high payload and good release	[9]
1 MHz, 2.0 W/cm^2 10% duty cycle	Optison	Bleomycin co-injected with MBs	Mouse squamose cell tumor model	Almost complete tumor regression after 4 weeks	[90]
3 MHz, 2 W/cm^2, duty cycle of 20% for 30 sec	Biodegradable diblock copolymers	0.75 mg/ml DOX encapsulated in MB	Mouse breast cancer model	Inhibition of tumor growth	[96,97]
1 MHz, of 270 Jcm^{-2}	Sonovue	Camptothecin in cell culture medium	HELA cell culture	LD_{50} of camptothecin is reduced from 58 to 18 nM	[99]

DOX: Doxorubicin; FITC: Fluorescein; HELA: HELA cell line; MB: Microbubble; MTX: Methotrexat; NBD: Nitrobenz-2-oxa-1,3-diazol-cholesterol; US: Ultrasound; UTMD: Ultrasound targeted microbubble destruction.

Table 4. Gene transfer outside the cardiovascular and musculoskeletal system.

Ultrasound conditions	Microbubbles	Gene	Target region	Results	Ref.
1 MHz, 0.55 MPa, 26% duty cycle, pulse repetition frequency 2 Hz	Optison	Luciferase plasmid DNA	Rat brain	Luciferase expression approximately tenfold increased compared to injection of naked plasmid DNA alone	[103]
1 MHz, 0.5 W/cm^2, duty cycle 20%, 5 sec	Optison	Luciferase plasmid DNA	Rat thoracic spinal cord	Successful and up to 60-fold higher transfer into the spinal cord without damage by UTMD	[104]
1 MHz, 1.8, 3 and 4 MPa	Optison	Human factor IX plasmid	Mouse liver	Up to 66-fold increase of factor IX expression	[129]
1 MHz, 5% power output, for a total of 60 sec at 30-sec intervals	Optison	Luciferase and GFP plasmid DNA	Rat kidney	UTMD enhanced the efficiency of gene transfer and expression in the rat kidney	[110]
1, 1.5, 2 and 3 W/cm^2, 120 sec, 50% duty cycle	Optison	Luciferase plasmid DNA	Rabbit cornea	UTMD greatly increases gene transfer to *in vivo* and *in vitro* corneal cells	[106]
1 MHz, 0.3 – 2.0 W/cm^2, 10 – 120 sec	Optison	Luciferase and GFP plasmid DNA	Rat intervertebral discs	Increase in luciferase and GFP activity for at least 24 weeks	[109]
1 MHZ for 30 sec	Optison	Smad 7 plasmid DNA	Mouse autoimmune crescentic glomerulonephritis model	Successful Smad7 gene transfer for 14 days improved proteinuria, renal function and pathology	[113]
1 MHz, 2 Wcm^{-2}, 20% duty cycle for 15 sec twice with a 75-sec interval	Optison	Smad 7 plasmid DNA	Rat intraperitoneal cavity	Gene expression was twofold increased	[111]
1.3 MHz, Mi 1.4	Phospholipid MBs	Betacellulin and pancreatic duodenal homeobox-1 plasmid DNA	Rat diabetes model	Sufficient pancreas targeted gene transfer to restore insulin production	[114]
1 MHz, 20 sec, 1.2 W/cm^2, duty cycle 50%	Liposome bubbles	GFP plasmid DNA	Rat ocular model	Improved gene transfer efficiency to rat subconjunctival tissue	[107]
1 MHz, 0.74 MPa, repetition frequency of 100 Hz and 20% duty cycle	Optison	Luciferase plasmid DNA	Mouse lung	Increased luciferase activity by 1.5 logs but lead to lung haemorrhages	[112]
950 kHz, 0.6 MPa duty ratio, 20%	Optison	Luciferase plasmid DNA	Mouse spinal cord	15-fold increased luciferase activity	[105]
1.17 MHz, 4.3 MPa, 20 cycle pulses, 60-sec exposure	Optison	Luciferase plasmid DNA	Mouse liver	Gene expression was increased up to 85-fold dependent on acoustic pressure over the range of 0 – 4.3 MPa, with a peak effect at 3 MPa	[108]
1 MHz; 3.0 W/cm^2	Optison, lipid microspheres	Herpes simplex thymidine kinase plasmid DNA	Mouse tumor model	Significant reduction in tumor volume in mice treated with herpes simplex thymidine kinase	[130]

GFP: Green fluorescent protein; MB: Microbubble; UTMD: Ultrasound targeted microbubble destruction.

optimal candidate for organ- or tissue-specific delivery. Microbubbles can be produced with various shell materials, are established for diagnostic procedures in humans, can be visualized by ultrasound with lower energies and can be locally destroyed by ultrasound with higher energies. In addition, the complicated process of acoustic reaction to the ultrasound field, such as non-linear oscillations and the development of high velocity fluid microjets, can transiently increase cell membrane or capillary permeability in the close vicinity of sonified microbubbles. Taking all these characteristics into account, ultrasound targeted destruction of loaded microbubbles seems to be an optimal technique for local drug and gene delivery. This has been shown by many proof of principle studies, especially in rodent models. However, several limitations of this technique have to be discussed. First, microbubbles are gas-filled microspheres. Thus, the payload of microbubbles is very limited. Bioactive substances can adhere to the shell or can form part of the shell. Both loading strategies are characterized by very low loading capacities. These can be increased if multilayers or additional oil layers are used. However, such microbubbles may significantly change their size and acoustic behaviour. Insufficient loading capacities can be circumvented by co-administration of the therapeutic substance with microbubbles. With this method, no limitations exist for the amount of bioactive substance. However, this strategy can only take advantage of transiently increased local permeability and not of local delivery. The second major limitation is related to potential side effects. While increased capillary permeability can be a therapeutic aim, excessive permeabilisation may lead to tissue damage and haemorrhage. Many studies have investigated potential side effects. Overall, side effects are a real risk but can be controlled by limiting microbubble concentration and ultrasound energy. This will have to be further investigated in large animal models.

7.2 Future prospects

Reviewing the literature, we can note that many proof of principle studies have been performed, mainly in small animals, demonstrating the potential of ultrasound targeted microbubble destruction as a site-specific, non-invasive therapeutic tool. However, large animal studies and studies in disease models are very rare. This fact is representative for the present state of UTMD. The difficulty in advancing this technique to preclinical studies lies in its low efficacy. While reporter gene assays are easy to perform and highly sensitive, therapeutic experiments, especially in large animals, need very efficient delivery of the therapeutic substance. There are two main strategies that can further improve this technique. First, new drug-specific microbubbles have to be designed that can load optimal amounts of the bioactive substance without losing their acoustic behaviour. Many researchers have shown activities in this field. Our improved understanding of microbubble behaviour helps in this process of pharmaceutical microbubble development. Second, optimal ultrasound modalities and machines have to be designed to improve the efficiency of microbubble destruction. Most studies have used ultrasound systems that are suboptimal for sonication of a whole organ. New three-dimensional ultrasound systems could destroy microbubbles in a larger portion of an organ, thus achieving more homogenous delivery and a higher rate of destroyed microbubbles per target organ. This would be an attractive challenge for the ultrasound industry.

In conclusion, ultrasound targeted microbubble destruction has been used in various organ systems and in tumours to successfully deliver drugs, proteins, gene therapy vectors and gene silencing constructs. Many proof of principle studies have demonstrated its potential as a non-invasive delivery tool. However, too few large animal studies and studies with therapeutic substances have been performed to see a clinical application of this technique in the near future. Nevertheless, there is great hope that preclinical large animal studies will confirm the successful results already obtained in small animals.

Acknowledgment

Raffi Bekeredjian is funded by the BioFuture grant of the Bundesministerium für Bildung und Forschung, Germany.

Bibliography

1. Tei C, Sakamaki T, Shah PM, et al. Myocardial contrast echocardiography: a reproducible technique of myocardial opacification for identifying regional perfusion deficits. Circulation 1983;67:585-93
2. Kuznetsova LA, Khanna S, Amso NN, et al. Cavitation bubble-driven cell and particle behavior in an ultrasound standing wave. J Acoust Soc Am 2005;117:104-12
3. Dollet B, van der Meer SM, Garbin V, et al. Nonspherical oscillations of ultrasound contrast agent microbubbles. Ultrasound Med Biol 2008;34:1465-73
4. Church CC, Allen JS. Mathematical models for contrast bubble dynamics. J Acoust Soc Am 2008;123:3111
5. Dalecki D; WFUMB Safety Symposium on Echo-Contrast Agents. bioeffects of ultrasound contrast agents in vivo. Ultrasound Med Biol 2007;33:205-13
6. Bull JL. The application of microbubbles for targeted drug delivery. Expert Opin Drug Deliv 2007;4:475-93
7. Klibanov AL. Microbubble contrast agents: targeted ultrasound imaging and ultrasound-assisted drug-delivery applications. Invest Radiol 2006;41:354-62
8. Postema M, Schmitz G. Ultrasonic bubbles in medicine: influence of the shell. Ultrason Sonochem 2007;14:438-44
9. Fang JY, Hung CF, Liao MH, et al. A study of the formulation design of acoustically active lipospheres as carriers for drug delivery. Eur J Pharm Biopharm 2007;67:67-75
10. May DJ, Allen JS, Ferrara KW. Dynamics and fragmentation of thick-shelled microbubbles. IEEE Trans Ultrason Ferroelectr Freq Control 2002;49:1400-10
11. El-Sherif DM, Wheatley MA. Development of a novel method for synthesis of a polymeric ultrasound contrast agent. J Biomed Mater Res A 2003;66:347-55
12. Narayan P, Marchant D, Wheatley MA. Optimization of spray drying by factorial design for production of hollow microspheres for ultrasound imaging. J Biomed Mater Res 2001;56:333-41
13. Smith MD, Elion JL, McClure RR, et al. Left heart opacification with peripheral venous injection of a new saccharide echo contrast agent in dogs. J Am Coll Cardiol 1989;13:1622-8
14. Smith MD, Kwan OL, Reiser HJ, et al. Superior intensity and reproducibility of SHU-454, a new right heart contrast agent. J Am Coll Cardiol 1984;3:992-8
15. Feinstein SB, Cheirif J, Ten Cate FJ, et al. Safety and efficacy of a new transpulmonary ultrasound contrast agent: initial multicenter clinical results. J Am Coll Cardiol 1990;16:316-24
16. Simon RH, Ho SY, D'Arrigo J, et al. Lipid-coated ultrastable microbubbles as a contrast agent in neurosonography. Invest Radiol 1990;25:1300-4
17. Schneider M, Broillet A, Bussat P, et al. Gray-scale liver enhancement in VX2 tumor-bearing rabbits using BR14, a new ultrasonographic contrast agent. Invest Radiol 1997;32:410-7
18. Meza M, Greener Y, Hunt R, et al. Myocardial contrast echocardiography: reliable, safe, and efficacious myocardial perfusion assessment after intravenous injections of a new echocardiographic contrast agent. Am Heart J 1996;132:871-81
19. Fritz TA, Unger EC, Sutherland G, et al. Phase I clinical trials of MRX-115. A new ultrasound contrast agent. Invest Radiol 1997;32:735-40
20. Porter TR, Xie F, Kricsfeld A, et al. Noninvasive identification of acute myocardial ischemia and reperfusion with contrast ultrasound using intravenous perfluoropropane-exposed sonicated dextrose albumin. J Am Coll Cardiol 1995;26:33-40
21. Forsberg F, Basude R, Liu JB, et al. Effect of filling gases on the backscatter from contrast microbubbles: theory and in vivo measurements. Ultrasound Med Biol 1999;25:1203-11
22. Pelura TJ. Clinical experience with AF0150 (Imagent US), a new ultrasound contrast agent. Acad Radiol 1998;5(Suppl 1):S69-71; discussion S72-4
23. Postema M, Bouakaz A, ten Cate FJ, et al. Nitric oxide delivery by ultrasonic cracking: some limitations. Ultrasonics 2006;44(Suppl 1):e109-13
24. Korpanty G, Grayburn PA, Shohet RV, et al. Targeting vascular endothelium with avidin microbubbles. Ultrasound Med Biol 2005;31:1279-83
25. Frenkel PA, Chen S, Thai T, et al. DNA-loaded albumin microbubbles enhance ultrasound-mediated transfection in vitro. Ultrasound Med Biol 2002;28:817-22
26. Lentacker I, De Geest BG, Vandenbroucke RE, et al. Ultrasound-responsive polymer-coated microbubbles that bind and protect DNA. Langmuir 2006;22:7273-8
27. Ferrara K, Pollard R, Borden M. Ultrasound microbubble contrast agents: fundamentals and application to gene and drug delivery. Ann Rev Biomed Eng 2007;9:415-47
28. Bekeredjian R, Grayburn PA, Shohet RV. Use of ultrasound contrast agents for gene or drug delivery in cardiovascular medicine. J Am Coll Cardiol 2005;45:329-35
29. Huber PE, Pfisterer P. In vitro and in vivo transfection of plasmid DNA in the Dunning prostate tumor R3327-AT1 is enhanced by focused ultrasound. Gene Ther 2000;7:1516-25
30. Seemann S, Hauff P, Schultze-Mosgau M, et al. Pharmaceutical evaluation of gas-filled microparticles as gene delivery system. Pharm Res 2002;19:250-7
31. Lum AF, Borden MA, Dayton PA, et al. Ultrasound radiation force enables targeted deposition of model drug carriers loaded on microbubbles. J Control Release 2006;111:128-34
32. Dufrene YBW, Green J, Lee G. Nanometerscale surface properties of mixed phopholipid monolayers and bilayers. Langmuir 1997;1:370-7
33. Mehier-Humbert S, Yan F, Frinking P, et al. Ultrasound-mediated gene delivery: influence of contrast agent on transfection. Bioconjug Chem 2007;18:652-62
34. Available from: http://www.ncbi.nlm.nih.gov/books/bookres.fcgi/micad/home.html
35. Unger EC, McCreery TP, Sweitzer RH, et al. Acoustically active lipospheres containing paclitaxel: a new therapeutic ultrasound contrast agent. Invest Radiol 1998;33:886-92
36. Borden MA, Caskey CF, Little E, et al. DNA and polylysine adsorption and multilayer construction onto cationic lipid-coated microbubbles. Langmuir 2007;23:9401-8
37. Muller OJ, Katus HA, Bekeredjian R. Targeting the heart with gene therapy-optimized gene delivery methods. Cardiovasc Res 2007;73:453-62

38. Dayton PA, Rychak JJ. Molecular ultrasound imaging using microbubble contrast agents. Front Biosci 2007;12:5124-42

39. Lindner JR, Coggins MP, Kaul S, et al. Microbubble persistence in the microcirculation during ischemia/reperfusion and inflammation is caused by integrin- and complement-mediated adherence to activated leukocytes. Circulation 2000;101:668-75

40. Lindner JR, Dayton PA, Coggins MP, et al. Noninvasive imaging of inflammation by ultrasound detection of phagocytosed microbubbles. Circulation 2000;102:531-8

41. Lindner JR, Song J, Xu F, et al. Noninvasive ultrasound imaging of inflammation using microbubbles targeted to activated leukocytes. Circulation 2000;102:2745-50

42. Christiansen JP, Leong-Poi H, Klibanov AL, et al. Noninvasive imaging of myocardial reperfusion injury using leukocyte-targeted contrast echocardiography. Circulation 2002;105:1764-67

43. Klibanov AL, Hughes MS, Villanueva FS, et al. Targeting and ultrasound imaging of microbubble-based contrast agents. Magma 1999;8:177-84

44. Borden MA, Sarantos MR, Stieger SM, et al. Ultrasound radiation force modulates ligand availability on targeted contrast agents. Mol Imaging 2006;5:139-47

45. Rovai D, Lombardi M, Cini G, et al. Echocardiographic contrast imaging of the human right heart: a multicenter study of the efficacy, safety, and reproducibility of intravenous SHU-454. J Clin Ultrasound 1991;19:523-30

46. Miller DL, Gies RA. Gas-body-based contrast agent enhances vascular bioeffects of 1.09 MHz ultrasound on mouse intestine. Ultrasound Med Biol 1998;24:1201-8

47. Miller DL, Gies RA. The influence of ultrasound frequency and gas-body composition on the contrast agent-mediated enhancement of vascular bioeffects in mouse intestine. Ultrasound Med Biol 2000;26:307-13

48. Miller DL, Quddus J. Diagnostic ultrasound activation of contrast agent gas bodies induces capillary rupture in mice. Proc Natl Acad Sci USA 2000;97:10179-84

49. Dalecki D, Raeman CH, Child SZ, et al. The influence of contrast agents on hemorrhage produced by lithotripter fields. Ultrasound Med Biol 1997;23:1435-9

50. Dalecki D, Raeman CH, Child SZ, et al. Hemolysis in vivo from exposure to pulsed ultrasound. Ultrasound Med Biol 1997;23:307-13

51. Meairs S, Alonso A. Ultrasound, microbubbles and the blood–brain barrier. Prog Biophys Mol Biol 2007;93:354-62

52. Kobayashi N, Yasu T, Yamada S, et al. Endothelial cell injury in venule and capillary induced by contrast ultrasonography. Ultrasound Med Biol 2002;28:949-56

53. Shohet RV, Chen S, Zhou YT, et al. Echocardiographic destruction of albumin microbubbles directs gene delivery to the myocardium. Circulation 2000;101:2554-6

54. Lawrie A, Brisken AF, Francis SE, et al. Microbubble-enhanced ultrasound for vascular gene delivery. Gene Ther 2000;7:2023-7

55. Taniyama Y, Tachibana K, Hiraoka K, et al. Development of safe and efficient novel nonviral gene transfer using ultrasound: enhancement of transfection efficiency of naked plasmid DNA in skeletal muscle. Gene Ther 2002;9:372-80

56. Kondo I, Ohmori K, Oshita A, et al. Treatment of acute myocardial infarction by hepatocyte growth factor gene transfer: the first demonstration of myocardial transfer of a 'functional' gene using ultrasonic microbubble destruction. J Am Coll Cardiol 2004;44:644-53

57. Li X, Wang Z, Ran H, et al. Experimental research on therapeutic angiogenesis induced by hepatocyte growth factor directed by ultrasound-targeted microbubble destruction in rats. J Ultrasound Med 2008;27:453-60

58. Korpanty G, Chen S, Shohet RV, et al. Targeting of VEGF-mediated angiogenesis to rat myocardium using ultrasonic destruction of microbubbles. Gene Ther 2005;12:1305-12

59. Zhigang W, Zhiyu L, Haitao R, et al. Ultrasound-mediated microbubble destruction enhances VEGF gene delivery to the infarcted myocardium in rats. Clin Imaging 2004;28:395-8

60. Leong-Poi H, Kuliszewski MA, Lekas M, et al. Therapeutic arteriogenesis by ultrasound-mediated VEGF165 plasmid gene delivery to chronically ischemic skeletal muscle. Circ Res 2007;101:295-303

61. Hashiya N, Aoki M, Tachibana K, et al. Local delivery of E2F decoy oligodeoxynucleotides using ultrasound with microbubble agent (Optison) inhibits intimal hyperplasia after balloon injury in rat carotid artery model. Biochem Biophys Res Commun 2004;317:508-14

62. Kipshidze NN, Porter TR, Dangas G, et al. Systemic targeted delivery of antisense with perflourobutane gas microbubble carrier reduced neointimal formation in the porcine coronary restenosis model. Cardiovasc Radiat Med 2003;4:152-9

63. Taniyama Y, Tachibana K, Hiraoka K, et al. Local delivery of plasmid DNA into rat carotid artery using ultrasound. Circulation 2002;105:1233-9

64. Zen K, Okigaki M, Hosokawa Y, et al. Myocardium-targeted delivery of endothelial progenitor cells by ultrasound-mediated microbubble destruction improves cardiac function via an angiogenic response. J Mol Cell Cardiol 2006;40:799-809

65. Iwasaki M, Adachi Y, Nishiue T, et al. Hepatocyte growth factor delivered by ultrasound-mediated destruction of microbubbles induces proliferation of cardiomyocytes and amelioration of left ventricular contractile function in Doxorubicin-induced cardiomyopathy. Stem Cells 2005;23:1589-97

66. Mukherjee D, Wong J, Griffin B, et al. Ten-fold augmentation of endothelial uptake of vascular endothelial growth factor with ultrasound after systemic administration. J Am Coll Cardiol 2000;35:1678-86

67. Bekeredjian R, Chen S, Grayburn PA, et al. Augmentation of cardiac protein delivery using ultrasound targeted microbubble destruction. Ultrasound Med Biol 2005;31:687-91

68. Pardridge WM. The blood–brain barrier: bottleneck in brain drug development. NeuroRx 2005;2:3-14

69. Lossinsky AS, Vorbrodt AW, Wisniewski HM. Scanning and transmission electron microscopic studies of microvascular pathology in the osmotically impaired blood-brain barrier. J Neurocytol 1995;24:795-806

70. Pan GY, Liu XD, Liu GQ. Intracarotid infusion of hypertonic mannitol changes permeability of blood–brain barrier to methotrexate in rats. Acta Pharmacol Sin 2000;21:613-6

71. Abbott NJ. Inflammatory mediators and modulation of blood–brain barrier permeability. Cell Mol Neurobiol 2000;20:131-47

72. Nomura T, Inamura T, Black KL. Intracarotid infusion of bradykinin selectively increases blood-tumor permeability in 9L and C6 brain tumors. Brain Res 1994;659:62-6

73. Inamura T, Nomura T, Bartus RT, et al. Intracarotid infusion of RMP-7, a bradykinin analog: a method for selective drug delivery to brain tumors. J Neurosurg 1994;81:752-8

74. Droste DW. Clinical utility of contrast-enhanced ultrasound in neurosonology. Eur Neurol 2008;59(Suppl 1):2-8

75. Vykhodtseva NI, Hynynen K, Damianou C. Histologic effects of high intensity pulsed ultrasound exposure with subharmonic emission in rabbit brain in vivo. Ultrasound Med Biol 1995;21:969-79

76. Hynynen K, McDannold N, Vykhodtseva N, et al. Noninvasive MR imaging-guided focal opening of the blood–brain barrier in rabbits. Radiology 2001;220:640-6

77. Hynynen K, McDannold N, Vykhodtseva N, et al. Focal disruption of the blood–brain barrier due to 260-kHz ultrasound bursts: a method for molecular imaging and targeted drug delivery. J Neurosurg 2006;105:445-54

78. McDannold N, Vykhodtseva N, Hynynen K. Effects of acoustic parameters and ultrasound contrast agent dose on focused-ultrasound induced blood-brain barrier disruption. Ultrasound Med Biol 2008;34:930-7

79. McDannold N, Vykhodtseva N, Hynynen K. Blood–brain barrier disruption induced by focused ultrasound and circulating preformed microbubbles appears to be characterized by the mechanical index. Ultrasound Med Biol 2008;34:834-40

80. Hynynen K, McDannold N, Sheikov NA, et al. Local and reversible blood–brain barrier disruption by noninvasive focused ultrasound at frequencies suitable for trans-skull sonications. Neuroimage 2005;24:12-20

81. Kinoshita M, McDannold N, Jolesz FA, et al. Targeted delivery of antibodies through the blood–brain barrier by MRI-guided focused ultrasound. Biochem Biophys Res Commun 2006;340:1085-90

82. Sheikov N, McDannold N, Vykhodtseva N, et al. Cellular mechanisms of the blood–brain barrier opening induced by ultrasound in presence of microbubbles. Ultrasound Med Biol 2004;30:979-89

83. Hynynen K, McDannold N, Vykhodtseva N, et al. Non-invasive opening of BBB by focused ultrasound. Acta Neurochir Suppl 2003;86:555-8

84. Treat LH, McDannold N, Vykhodtseva N, et al. Targeted delivery of doxorubicin to the rat brain at therapeutic levels using MRI-guided focused ultrasound. Int J Cancer 2007;121:901-7

85. Yang FY, Fu WM, Yang RS, et al. Quantitative evaluation of focused ultrasound with a contrast agent on blood–brain barrier disruption. Ultrasound Med Biol 2007;33:1421-7

86. Choi JJ, Pernot M, Brown TR, et al. Spatio-temporal analysis of molecular delivery through the blood-brain barrier using focused ultrasound. Phys Med Biol 2007;52:5509-30

87. Choi JJ, Pernot M, Small SA, et al. Noninvasive, transcranial and localized opening of the blood–brain barrier using focused ultrasound in mice. Ultrasound Med Biol 2007;33:95-104

88. Song J, Chappell JC, Qi M, et al. Influence of injection site, microvascular pressure and ultrasound variables on microbubble-mediated delivery of microspheres to muscle. J Am Coll Cardiol 2002;39:726-31

89. Price RJ, Skyba DM, Kaul S, et al. Delivery of colloidal particles and red blood cells to tissue through microvessel ruptures created by targeted microbubble destruction with ultrasound. Circulation 1998;98:1264-7

90. Iwanaga K, Tominaga K, Yamamoto K, et al. Local delivery system of cytotoxic agents to tumors by focused sonoporation. Cancer Gene Ther 2007;14:354-63

91. Shortencarier MJ, Dayton PA, Bloch SH, et al. A method for radiation-force localized drug delivery using gas-filled lipospheres. IEEE Trans Ultrason Ferroelectr Freq Control 2004;51:822-31

92. Ho SY, Barbarese E, D'Arrigo JS, et al. Evaluation of lipid-coated microbubbles as a delivery vehicle for Taxol in brain tumor therapy. Neurosurgery 1997;40:1260-6; discussion 1266-8

93. Tartis MS, McCallan J, Lum AF, et al. Therapeutic effects of paclitaxel-containing ultrasound contrast agents. Ultrasound Med Biol 2006;32:1771-80

94. Kheirolomoom A, Dayton PA, Lum AF, et al. Acoustically active microbubbles conjugated to liposomes: characterization of a proposed drug delivery vehicle. J Control Release 2007;118:275-84

95. Shive MS, Anderson JM. Biodegradation and biocompatibility of PLA and PLGA microspheres. Adv Drug Deliv Rev 1997;28:5-24

96. Rapoport N, Gao Z, Kennedy A. Multifunctional nanoparticles for combining ultrasonic tumor imaging and targeted chemotherapy. J Natl Cancer Inst 2007;99:1095-106

97. Gao Z, Kennedy AM, Christensen DA, et al. Drug-loaded nano/microbubbles for combining ultrasonography and targeted chemotherapy. Ultrasonics 2007;48:260-70

98. Gao Z, Fain HD, Rapoport N. Ultrasound-enhanced tumor targeting of polymeric micellar drug carriers. Mol Pharm 2004;1:317-30

99. Li YS, Reid CN, McHale AP. Enhancing ultrasound-mediated cell membrane permeabilisation (sonoporation) using a high frequency pulse regime and implications for ultrasound-aided cancer chemotherapy. Cancer Lett 2008;266:156-62

100. Bekeredjian R, Kroll RD, Fein E, et al. Ultrasound Targeted Microbubble Destruction Increases Capillary Permeability in Hepatomas. Ultrasound Med Biol 2007;33:1592-8

101. Stieger SM, Caskey CF, Adamson RH, et al. Enhancement of vascular permeability with low-frequency contrast-enhanced ultrasound in the chorioallantoic membrane model. Radiology 2007;243:112-21

102. Sonoda S, Tachibana K, Uchino E, et al. Inhibition of melanoma by ultrasound-microbubble-aided drug delivery suggests membrane permeabilization. Cancer Biol Ther 2007;6:1276-83

103. Shimamura M, Sato N, Taniyama Y, et al. Development of efficient plasmid DNA transfer into adult rat central nervous system using microbubble-enhanced ultrasound. Gene Ther 2004;11:1532-9

104. Shimamura M, Sato N, Taniyama Y, et al. Gene transfer into adult rat spinal cord using naked plasmid DNA and ultrasound

microbubbles. J Gene Med 2005;7:1468-74

105. Takahashi M, Kido K, Aoi A, et al. Spinal gene transfer using ultrasound and microbubbles. J Control Release 2007;117:267-72
106. Sonoda S, Tachibana K, Uchino E, et al. Gene transfer to corneal epithelium and keratocytes mediated by ultrasound with microbubbles. Invest Ophthalmol Vis Sci 2006;47:558-64
107. Yamashita T, Sonoda S, Suzuki R, et al. A novel bubble liposome and ultrasound-mediated gene transfer to ocular surface: RC-1 cells in vitro and conjunctiva in vivo. Exp Eye Res 2007;85:741-8
108. Shen ZP, Brayman AA, Chen L, et al. Ultrasound with microbubbles enhances gene expression of plasmid DNA in the liver via intraportal delivery. Gene Ther 2008;15:1147-55
109. Nishida K, Doita M, Takada T, et al. Sustained transgene expression in intervertebral disc cells in vivo mediated by microbubble-enhanced ultrasound gene therapy. Spine 2006;31:1415-9
110. Koike H, Tomita N, Azuma H, et al. An efficient gene transfer method mediated by ultrasound and microbubbles into the kidney. J Gene Med 2005;7:108-16
111. Guo H, Leung JC, Chan LY, et al. Ultrasound-contrast agent mediated naked gene delivery in the peritoneal cavity of adult rat. Gene Ther 2007;14:1712-20
112. Xenariou S, Griesenbach U, Liang HD, et al. Use of ultrasound to enhance nonviral lung gene transfer in vivo. Gene Ther 2007;14:768-74
113. Ka SM, Huang XR, Lan HY, et al. Smad7 gene therapy ameliorates an autoimmune crescentic glomerulonephritis in mice. J Am Soc Nephrol 2007;18:1777-88
114. Chen S, Ding J, Yu C, et al. Reversal of streptozotocin-induced diabetes in rats by gene therapy with betacellulin and pancreatic duodenal homeobox-1. Gene Ther 2007;14:1102-10
115. Vannan M, McCreery T, Li P, et al. Ultrasound-mediated transfection of canine myocardium by intravenous administration of cationic microbubble-linked plasmid DNA. J Am Soc Echocardiogr 2002;15:214-8
116. Teupe C, Richter S, Fisslthaler B, et al. Vascular gene transfer of phosphomimetic endothelial nitric oxide synthase (S1177D) using ultrasound-enhanced destruction of plasmid-loaded microbubbles improves vasoreactivity. Circulation 2002;105:1104-9
117. Chen S, Shohet RV, Bekeredjian R, et al. Optimization of ultrasound parameters for cardiac gene delivery of adenoviral or plasmid deoxyribonucleic acid by ultrasound-targeted microbubble destruction. J Am Coll Cardiol 2003;42:301-8
118. Bekeredjian R, Chen S, Frenkel PA, et al. Ultrasound-targeted microbubble destruction can repeatedly direct highly specific plasmid expression to the heart. Circulation 2003;108:1022-6
119. Pislaru SV, Pislaru C, Kinnick RR, et al. Optimization of ultrasound-mediated gene transfer: comparison of contrast agents and ultrasound modalities. Eur Heart J 2003;24:1690-8
120. Christiansen JP, French BA, Klibanov AL, et al. Targeted tissue transfection with ultrasound destruction of plasmid-bearing cationic microbubbles. Ultrasound Med Biol 2003;29:1759-67
121. Li T, Tachibana K, Kuroki M. Gene transfer with echo-enhanced contrast agents: comparison between Albunex, Optison, and Levovist in mice – initial results. Radiology 2003;229:423-8
122. Lu QL, Liang HD, Partridge T, et al. Microbubble ultrasound improves the efficiency of gene transduction in skeletal muscle in vivo with reduced tissue damage. Gene Ther 2003;10:396-405
123. Erikson JM, Freeman GL, Chandrasekar B. Ultrasound-targeted antisense oligonucleotide attenuates ischemia/reperfusion-induced myocardial tumor necrosis factor-alpha. J Mol Cell Cardiol 2003;35:119-30
124. Guo DP, Li XY, Sun P, et al. Ultrasound/microbubble enhances foreign gene expression in ECV304 cells and murine myocardium. Acta Biochim Biophys Sin (Shanghai) 2004;36:824-31
125. Tsunoda S, Mazda O, Oda Y, et al. Sonoporation using microbubble BR14 promotes pDNA/siRNA transduction to murine heart. Biochem Biophys Res Commun 2005;336:118-27
126. Wang X, Liang HD, Dong B, et al. Gene transfer with microbubble ultrasound and plasmid DNA into skeletal muscle of mice: comparison between commercially available microbubble contrast agents. Radiology 2005;237:224-9
127. Akowuah EF, Gray C, Lawrie A, et al. Ultrasound-mediated delivery of TIMP-3 plasmid DNA into saphenous vein leads to increased lumen size in a porcine interposition graft model. Gene Ther 2005;12:1154-7
128. Nakaya H, Shimizu T, Isobe K, et al. Microbubble-enhanced ultrasound exposure promotes uptake of methotrexate into synovial cells and enhanced anti-inflammatory effects in the knees of rabbits with antigen-induced arthritis. Arthritis Rheum 2005;52:2559-66
129. Miao CH, Brayman AA, Loeb KR, et al. Ultrasound enhances gene delivery of human factor IX plasmid. Hum Gene Ther 2005;16:893-905
130. Aoi A, Watanabe Y, Mori S, et al. Herpes simplex virus thymidine kinase-mediated suicide gene therapy using nano/microbubbles and ultrasound. Ultrasound Med Biol 2008;34:425-34

Affiliation

Christian R Mayer MD, Nicolas A Geis MD, Hugo A Katus MD & Raffi Bekeredjian† MD
†Author for correspondence
University of Heidelberg,
Department of Internal Medicine III,
Im Neuenheimer Feld 410,
69120 Heidelberg, Germany
Tel: +49 0 6221 5639097;
Fax: +49 0 6221 565515;
E-mail: raffi.bekeredjian@med.uni-heidelberg.de